Computer Physics Communications 180 (2009) 2348–2354

Contents lists available at ScienceDirect

Computer Physics Communications

www.elsevier.com/locate/cpc

Scattering of electromagnetic radiation by a multilayered sphere ☆

O. Peña *, U. Pal

Instituto de Física, Universidad Autónoma de Puebla, Apartado Postal J-48, Puebla, Puebla 72570, Mexico

ARTICLE INFO

Article history:
Received 25 July 2008
Received in revised form 1 July 2009
Accepted 23 July 2009
Available online 29 July 2009

PACS:
01.50.hv
42.25.-p
42.25.Bs
42.25.Fx

Keywords:
Mie scattering
Multilayered sphere
Efficiency factors
Cross-sections

ABSTRACT

The computer implementation of the algorithm for the calculation of electromagnetic radiation scattering by a multilayered sphere developed by Yang, is presented. It has been shown that the program is effective, resulting in very accurate values of scattering efficiencies for a wide range of size parameters, which is a considerable improvement over previous implementations of similar algorithms. The program, named *scattnlay*, would be the first of its kind to be publicly available.

Program summary

Program title: scattnlay
Catalogue identifier: AEEY_v1_0
Program summary URL: http://cpc.cs.qub.ac.uk/summaries/AEEY_1_0.html
Program obtainable from: CPC Program Library, Queen's University, Belfast, N. Ireland
Licensing provisions: Gnu General Public License (GPL)
No. of lines in distributed program, including test data, etc.: 8932
No. of bytes in distributed program, including test data, etc.: 175 276
Distribution format: tar.gz
Programming language: ANSI C
Computer: Any with a C compiler
Operating system: Linux (any), Windows, Solaris
RAM: ∼1–100 MB
Classification: 1.3
Nature of problem: The scattering of electromagnetic (EM) radiation by a multilayered sphere is an interesting phenomenon to study for the application of such materials in several fields. Just to mention two examples, metal nanoshells (a dielectric core surrounded by a metallic shell) are a class of nanoparticles with tunable optical resonances that can be used, among others, in medicine for optical imaging and photothermal cancer therapy; while in the field of atmospheric sciences, light absorption by aerosols has a heating effect in the atmosphere that is of great interest to study several climatic effects. Although at first glance the expressions of the scattering coefficients seem simple and straightforward to implement, they involve several numerical difficulties which make most of the existent algorithms inapplicable to several extreme cases. More recently, Yang [1] has developed an improved recursive algorithm that circumvents most of the numerical problems present in previous algorithms, which is implemented in the current program.
Solution method: Calculations of Mie scattering coefficients and efficiency factors for a multilayered sphere as described by Yang [1], combined with standard solutions of the scattering amplitude functions.
Restrictions: Single scattering, permeability of the layers is always unity.
Running time: Seconds to minutes
References:
[1] W. Yang, Appl. Opt. 42 (2003) 1710–1720.

1. Introduction

The scattering of electromagnetic (EM) radiation by a multilayered sphere is an interesting phenomenon to study for the application of such materials in several fields. Just to mention two exam-

☆ This paper and its associated computer program are available via the Computer Physics Communications homepage on ScienceDirect (http://www.sciencedirect.com/science/journal/00104655).

* Corresponding author.
E-mail address: ovidio@bytesfall.com (O. Peña).

0010-4655/$ – see front matter
doi:10.1016/j.cpc.2009.07.010

ples, metal nanoshells (a dielectric core surrounded by a metallic shell) are a class of nanoparticles with tunable optical resonances that can be used, among others, in medicine for optical imaging and photothermal cancer therapy [1–3]; while in the field of atmospheric sciences, light absorption by aerosols has a heating effect in the atmosphere that is of great interest to study several climatic effects [4,5].

The first model developed to study the EM scattering by a coated sphere was given by Aden and Kerker [6] and, after that, Wait [7] proposed a recursive algorithm applicable to the multilayered sphere and more recently, Bhandari [8] proposed a complete set of scattering coefficients for the latter case. Although at first glance the expressions of the scattering coefficients seem simple and straightforward to implement, they involve several numerical difficulties which make most of the existent algorithms [7,9–11] inapplicable to several cases [12,13]. A few years ago, Yang [14] developed an improved recursive algorithm that circumvents most of the numerical problems present in previous algorithms, and although the development of a computer program that implements the algorithm has already been reported [15], it is not publicly available.

In this article, a computer program based on the calculation of the Mie coefficients and efficiency factors for single multilayered spheres as described in Yang's algorithm [14] is presented and its exactitude has been successfully tested for several cases.

2. EM scattering by a multilayered sphere

In short, the solution of the scattering by a multilayered sphere consists in expressing the EM fields in each layer l in terms of appropriate sets of spherical wave functions. Each layer is characterized by a size parameter $x_l = 2\pi N_m r_l/\lambda = kr_l$ and a relative refractive index $m_l = N_l/N_m$, $l = 1, 2, \ldots, L$, where λ is the wavelength of the incident wave in vacuum, r_l is the outer radius of the lth layer, N_m and N_l are the refractive index of the medium outside the particle and its lth component, respectively, and k is the propagation constant. In the region outside the particle, the relative refractive index is $m_{L+1} = 1$. It is supposed that the incident electric field is an x-polarized wave, $\vec{E}_i = E_0 \exp[ikr\cos(\theta)]\hat{e}_x$ with a time dependence of $\exp(-i\omega t)$. The space is divided into two regions: the region inside the multilayered sphere, and the surrounding medium outside the particle. The electric and magnetic fields (inside and outside the sphere) are considered as the superposition of sets of spherical wave functions. For example, $\vec{E}_{in}$ and $\vec{E}_{out}$ can be expressed in terms of complex spherical eigenvectors [14]:

$$\vec{E}_{in} = \sum_{n=1}^{\infty} E_n\left[c_n^{(l)}\vec{M}_{o1n}^{(1)} - id_n^{(l)}\vec{N}_{e1n}^{(1)}\right], \tag{1}$$

$$\vec{E}_{out} = \sum_{n=1}^{\infty} E_n\left[ia_n^{(l)}\vec{N}_{e1n}^{(3)} - b_n^{(l)}\vec{M}_{o1n}^{(3)}\right], \tag{2}$$

where $E_n = i^n E_0(2n+1)/n(n+1)$, and $\vec{M}_{o1n}^{(j)}$ and $\vec{N}_{e1n}^{(j)}$ $(j = 1, 3)$ are the vector harmonic functions with the radial dependence of the first kind of spherical Bessel function for $j = 1$ and the first kind of spherical Hankel function for $j = 3$ (the explicit expressions for $\vec{M}_{o1n}^{(j)}$ and $\vec{N}_{e1n}^{(j)}$ can be found elsewhere, for instance, in Chapter 4 of Ref. [18]).

In the region outside the sphere, the total external field is the superposition of the incident and scattered fields, $\vec{E} = \vec{E}_i + \vec{E}_s$, which can be expanded by:

$$\vec{E}_i = \sum_{n=1}^{\infty} E_n\left[\vec{M}_{o1n}^{(1)} - i\vec{N}_{e1n}^{(1)}\right], \tag{3}$$

$$\vec{E}_s = \sum_{n=1}^{\infty} E_n\left[ia_n\vec{N}_{e1n}^{(3)} - b_n\vec{M}_{o1n}^{(3)}\right], \tag{4}$$

where a_n and b_n are the scattering coefficients. It can be deduced [14] that $a_n^{(1)} = b_n^{(1)} = 0$, and $c_n^{(L+1)} = d_n^{(L+1)} = 1$. The expansion coefficients ($a_n^{(l)}$, $b_n^{(l)}$, $c_n^{(l)}$, and $d_n^{(l)}$) and scattering coefficients (a_n and b_n) are obtained by matching the tangential components of EM fields at each interface and after a little bit of algebra (for details see Ref. [14]), the final coefficients in the series can be identified with the scattering coefficients [14]:

$$a_n = a_n^{L+1} = \frac{[H_n^a(m_L x_L)/m_L + n/x_L]\psi_n(x_L) - \psi_{n-1}(x_L)}{[H_n^a(m_L x_L)/m_L + n/x_L]\zeta_n(x_L) - \zeta_{n-1}(x_L)}, \tag{5}$$

$$b_n = b_n^{L+1} = \frac{[m_L H_n^b(m_L x_L) + n/x_L]\psi_n(x_L) - \psi_{n-1}(x_L)}{[m_L H_n^b(m_L x_L) + n/x_L]\zeta_n(x_L) - \zeta_{n-1}(x_L)}, \tag{6}$$

where, ψ_n and ζ_n are the Riccati–Bessel functions (as defined in Ref. [13]) and the determinants H_n^a and H_n^b can be calculated by the expressions [14]:

$$H_n^a(m_1 x_1) = D_n^{(1)}(m_1 x_1), \tag{7a}$$

$$H_n^a(m_l x_l) = \frac{G_2 D_n^{(1)}(m_l x_l) - Q_n^{(l)} G_1 D_n^{(3)}(m_l x_l)}{G_2 - Q_n^{(l)} G_1}, \quad l = 2, \ldots, L, \tag{7b}$$

$$H_n^b(m_1 x_1) = D_n^{(1)}(m_1 x_1), \tag{8a}$$

$$H_n^b(m_l x_l) = \frac{\tilde{G}_2 D_n^{(1)}(m_l x_l) - Q_n^{(l)} \tilde{G}_1 D_n^{(3)}(m_l x_l)}{\tilde{G}_2 - Q_n^{(l)} \tilde{G}_1}, \quad l = 2, \ldots, L, \tag{8b}$$

and

$$D_n^{(1)}(z) = \psi_n'(z)/\psi_n(z), \tag{9}$$

$$D_n^{(3)}(z) = \zeta_n'(z)/\zeta_n(z), \tag{10}$$

$$Q_n^{(l)} = \frac{\psi_n(m_l x_{l-1})}{\zeta_n(m_l x_{l-1})} \Big/ \frac{\psi_n(m_l x_l)}{\zeta_n(m_l x_l)}, \tag{11}$$

$$G_1 = m_l H_n^a(m_{l-1} x_{l-1}) - m_{l-1} D_n^{(1)}(m_l x_{l-1}), \tag{12}$$

$$G_2 = m_l H_n^a(m_{l-1} x_{l-1}) - m_{l-1} D_n^{(3)}(m_l x_{l-1}), \tag{13}$$

$$\tilde{G}_1 = m_{l-1} H_n^b(m_{l-1} x_{l-1}) - m_l D_n^{(1)}(m_l x_{l-1}), \tag{14}$$

$$\tilde{G}_2 = m_{l-1} H_n^b(m_{l-1} x_{l-1}) - m_l D_n^{(3)}(m_l x_{l-1}). \tag{15}$$

One important thing to have into consideration with the current algorithm (and indeed with all existent algorithms known to us) is that there exists a possibility of failure due to zero denominators. For example, $j_n(z)$ has real zeros, leading to poles of $D_n^{(1)}(z)$, and $h_n^{(1)}(z)$ has complex zeros, leading to poles of $D_n^{(3)}(z)$. Additionally, Cachorro and Salcedo [16] have shown that there may also be the possibility of isolated singularities in the amplitudes $a_n^{(l)}$ and $b_n^{(l)}$ of the spherical vector waves, fortunately they are so narrow that they will not normally show up [16].

2.1. Computational algorithm

Before we can calculate the scattering coefficients, it is necessary to determine the logarithmic derivatives of the Riccati–Bessel functions ($D_n^{(1)}(z)$ and $D_n^{(3)}(z)$), the ratio $Q_n^{(l)}$, $\psi_n(x_L)$ and $\zeta_n(x_L)$. Firstly $D_n^{(1)}(z)$, this is the same that was used before in the algorithms of the original Mie theory; Wiscombe [17] showed that it can be accurately calculated by the use of a downward recurrence:

$$D^{(1)}_{N_{max}}(z) = 0 + i0, \tag{16a}$$

$$D^{(1)}_{n-1}(z) = \frac{n}{z} - \frac{1}{D^{(1)}_n(z) + n/z}, \quad n = N_{max}, \ldots, 1. \tag{16b}$$

The number of terms, N_{max}, is a function of the size parameters. A good choice [17] for the number of terms is given by $N_{max} = \max(N_{stop}, |m_l x_l|, |m_l x_{l-1}|) + 15$, $l = 1, 2, \ldots, L$. The value of N_{stop} is the integer closest to:

$$N_{stop} = \left\{ \begin{array}{ll} x_L + 4x_L^{1/3} + 1, & 0.02 \leqslant x_L < 8, \\ x_L + 4.05x_L^{1/3} + 2, & 8 \leqslant x_L < 4200, \\ x_L + 4x_L^{1/3} + 2, & 4200 \leqslant x_L < 20{,}000. \end{array} \right\} \tag{17}$$

For the case of $D^{(3)}_n(z)$, Mackowski et al. [9] have shown that it is possible to calculate it using the following method, which is stable for all values of z:

$$\psi_0(z)\zeta_0(z) = \frac{1}{2}\big[1 - (\cos 2a + i \sin 2a)\exp(-2b)\big], \tag{18a}$$

$$D^{(3)}_0(z) = i, \tag{18b}$$

$$\psi_n(z)\zeta_n(z) = \psi_{n-1}(z)\zeta_{n-1}(z) \times \left[\frac{n}{z} - D^{(1)}_{n-1}(z)\right]\left[\frac{n}{z} - D^{(3)}_{n-1}(z)\right], \tag{18c}$$

$$D^{(3)}_n(z) = D^{(1)}_n(z) + \frac{i}{\psi_n(z)\zeta_n(z)}, \quad n = 1, \ldots, N_{max}, \tag{18d}$$

where $z = a + ib$. The ratio $Q^{(l)}_n$ can be accurately determined by [14]:

$$Q^{(l)}_0 = \frac{\exp(-i2a_1) - \exp(-2b_1)}{\exp(-i2a_2) - \exp(-2b_2)} \times \exp\big(-2[b_2 - b_1]\big), \tag{19a}$$

$$Q^{(l)}_n = Q^{(l)}_{n-1}\left(\frac{x_{l-1}}{x_l}\right)^2 \frac{[z_2 D^{(1)}_n(z_2) + n]}{[z_1 D^{(1)}_n(z_1) + n]} \frac{[n - z_2 D^{(3)}_{n-1}(z_2)]}{[n - z_1 D^{(3)}_{n-1}(z_1)]}, \quad n = 1, \ldots, N_{max}, \tag{19b}$$

where $z_1 = m_l x_{l-1} = a_1 + ib_1$ and $z_2 = m_l x_l = a_2 + ib_2$. Finally, $\psi_n(x_L)$ and $\zeta_n(x_L)$ are also the same functions used in most of the algorithms for the scattering by a solid sphere and can be calculated from [9,17]:

$$\psi_0(x_L) = \sin(x_L), \tag{20a}$$

$$\psi_n(x_L) = \psi_{n-1}(x_L)\left[\frac{n}{x_L} - D^{(1)}_{n-1}(x_L)\right], \quad n = 1, \ldots, N_{max}, \tag{20b}$$

$$\zeta_0(x_L) = \sin(x_L) - i\cos(x_L), \tag{21a}$$

$$\zeta_n(x_L) = \zeta_{n-1}(x_L)\left[\frac{n}{x_L} - D^{(3)}_{n-1}(x_L)\right], \quad n = 1, \ldots, N_{max}. \tag{21b}$$

Once the above mentioned quantities for x_L, z_1 and z_2 are determined, it is possible to use the expressions (5)–(15) to calculate the scattering coefficients and after that we are ready to obtain all the measurable quantities associated with scattering and absorption, such as scattering matrix elements and efficiency factors.

2.2. Scattering matrix

Now, let the radiation be described by the four-component Stokes vector: $\hat{I} = [I, Q, U, V]^T$. The relation between the incident and scattered Stokes parameters is given by the scattering matrix $\hat{S}$ [18]:

$$\hat{I}_s \propto \hat{S}\hat{I}_i, \tag{22}$$

where $\hat{I}_i(\hat{I}_s)$ is the Stokes vector before (after) the scattering and:

$$\hat{S}(\theta) = \begin{bmatrix} S_{11}(\theta) & S_{12}(\theta) & 0 & 0 \\ S_{12}(\theta) & S_{11}(\theta) & 0 & 0 \\ 0 & 0 & S_{33}(\theta) & S_{34}(\theta) \\ 0 & 0 & -S_{34}(\theta) & S_{33}(\theta) \end{bmatrix}, \tag{23}$$

here θ is the scattering angle (angle between the direction of the incident and the scattered radiation). The elements of the scattering matrix S_{ik} can be derived from the complex scattering amplitudes (the asterisk denotes the complex conjugation) $S_1(\theta), S_2(\theta)$:

$$S_{11}(\theta) = \tfrac{1}{2}\big[|S_2(\theta)|^2 + |S_1(\theta)|^2\big], \tag{24a}$$

$$S_{12}(\theta) = \tfrac{1}{2}\big[|S_2(\theta)|^2 - |S_1(\theta)|^2\big], \tag{24b}$$

$$S_{33}(\theta) = \tfrac{1}{2}\big[S_1(\theta)S_2^*(\theta) + S_1^*(\theta)S_2(\theta)\big], \tag{24c}$$

$$S_{34}(\theta) = \tfrac{i}{2}\big[S_1(\theta)S_2^*(\theta) - S_1^*(\theta)S_2(\theta)\big]. \tag{24d}$$

The scattering amplitudes, in turn, can be calculated as:

$$S_1(\theta) = \sum_{n=1}^{\infty} \frac{2n+1}{n(n+1)}\big[a_n\pi_n(\theta) + b_n\tau_n(\theta)\big], \tag{25a}$$

$$S_2(\theta) = \sum_{n=1}^{\infty} \frac{2n+1}{n(n+1)}\big[a_n\tau_n(\theta) + b_n\pi_n(\theta)\big]. \tag{25b}$$

The angular functions π_n and τ_n only depend on $\cos(\theta)$ and can be found from recurrence relations [17]:

$$\pi_0(\theta) = 0, \qquad \pi_1(\theta) = 1, \tag{26a}$$

$$\pi_n(\theta) = \frac{2n-1}{n-1}\cos(\theta)\pi_{n-1}(\theta) - \frac{n}{n-1}\pi_{n-2}(\theta) \quad (n \geqslant 2), \tag{26b}$$

$$\tau_n(\theta) = n\cos(\theta)\pi_n(\theta) - (n+1)\pi_{n-1}(\theta) \quad (n \geqslant 1). \tag{26c}$$

2.3. Efficiency factors

The extinction, scattering and radiation pressure efficiency factors (Q_{ext}, Q_{sca} and Q_{pr}) are readily obtained by the relations [18]:

$$Q_{ext} = \frac{2}{x_L^2}\sum_{n=1}^{\infty}(2n+1)\,\mathrm{Re}\{a_n + b_n\}, \tag{27}$$

$$Q_{sca} = \frac{2}{x_L^2}\sum_{n=1}^{\infty}(2n+1)\big(|a_n|^2 + |b_n|^2\big), \tag{28}$$

$$Q_{pr} = Q_{ext} - gQ_{sca} = Q_{ext} - \frac{4}{x_L^2}\left\{\sum_{n=1}^{\infty}\left[\frac{n(n+2)}{n+1}\,\mathrm{Re}\big\{a_n a_{n+1}^* + b_n b_{n+1}^*\big\} + \frac{2n+1}{n(n+1)}\,\mathrm{Re}\big\{a_n b_n^*\big\}\right]\right\}. \tag{29}$$

From the calculated efficiencies it is also possible to derive the absorption efficiency factor (Q_{abs}), single scattering albedo (Λ) and asymmetry parameter (g):

$$Q_{abs} = Q_{ext} - Q_{sca}, \tag{30}$$

$$\Lambda = Q_{sca}/Q_{ext}, \tag{31}$$

$$g = (Q_{ext} - Q_{pr})/Q_{sca}. \tag{32}$$

Yet another quantity, which is mainly relevant to the radar community, is the radar backscattering efficiency factor (Q_{bk}) [18]:

$$Q_{bk} = \frac{1}{x_L^2}\left|\sum_{n=1}^{\infty}(2n+1)(-1)^n(a_n - b_n)\right|^2. \tag{33}$$

For all the efficiency factors, it can be found the corresponding cross sections from the relation $C = AQ$, where $A = \pi r_L^2$ is the geometrical cross-section of the particle.

Finally, one more useful quantity which can be calculated is the differential (bistatic) scattering cross section $dC_{sca}/d\Omega$, defined as the energy scattered per unit time into a unit solid angle about a direction defined by the scattering angle θ for unit incident irradiance. It is expressed in terms of the scattered irradiance $I_s(\theta)$, the incident irradiance I_i, and the distance r to the detector as [18,19]:

$$\frac{dC_{sca}}{d\Omega} = \frac{r^2 I_s(\theta)}{I_i} = \frac{1}{k^2}\left[S_{11}(\theta) + \frac{Q_i}{I_i} S_{12}(\theta)\right]. \tag{34}$$

3. Computer program

The presented program (*scattnlay*) is written in ANSI C. In order to offer more flexibility the program was divided in three files: the main program (*scattnlay.c*) is responsible for the input/output of the data, the library *nmie.c* is the actual implementation of Yang's algorithm and the library *ucomplex.c* provides the functions needed for the complex algebra. With this distribution it is possible to use the scattering code either as a standalone program or as a library for inclusion into some other program. In the file *nmie.c* the only exported function is *nMie*, which performs the actual calculation. It receives five parameters: *L*, the number of layers; *x*, an array containing the size parameters of the layers [*1..L*]; *m*, an array containing the relative refractive indexes of the layers [*1..L*]; nTheta, the number of scattering angles and Theta, and array containing the angles θ (in degrees) at which the scattering amplitudes will be calculated. The output of the function consists of the seven parameters described in Eqs. (27)–(33) and the two complex scattering amplitudes [Eqs. (25a) and (25b)], and returns an integer, which is the number of multipolar expansion terms used for the calculations. Neither the elements of the scattering matrix nor the

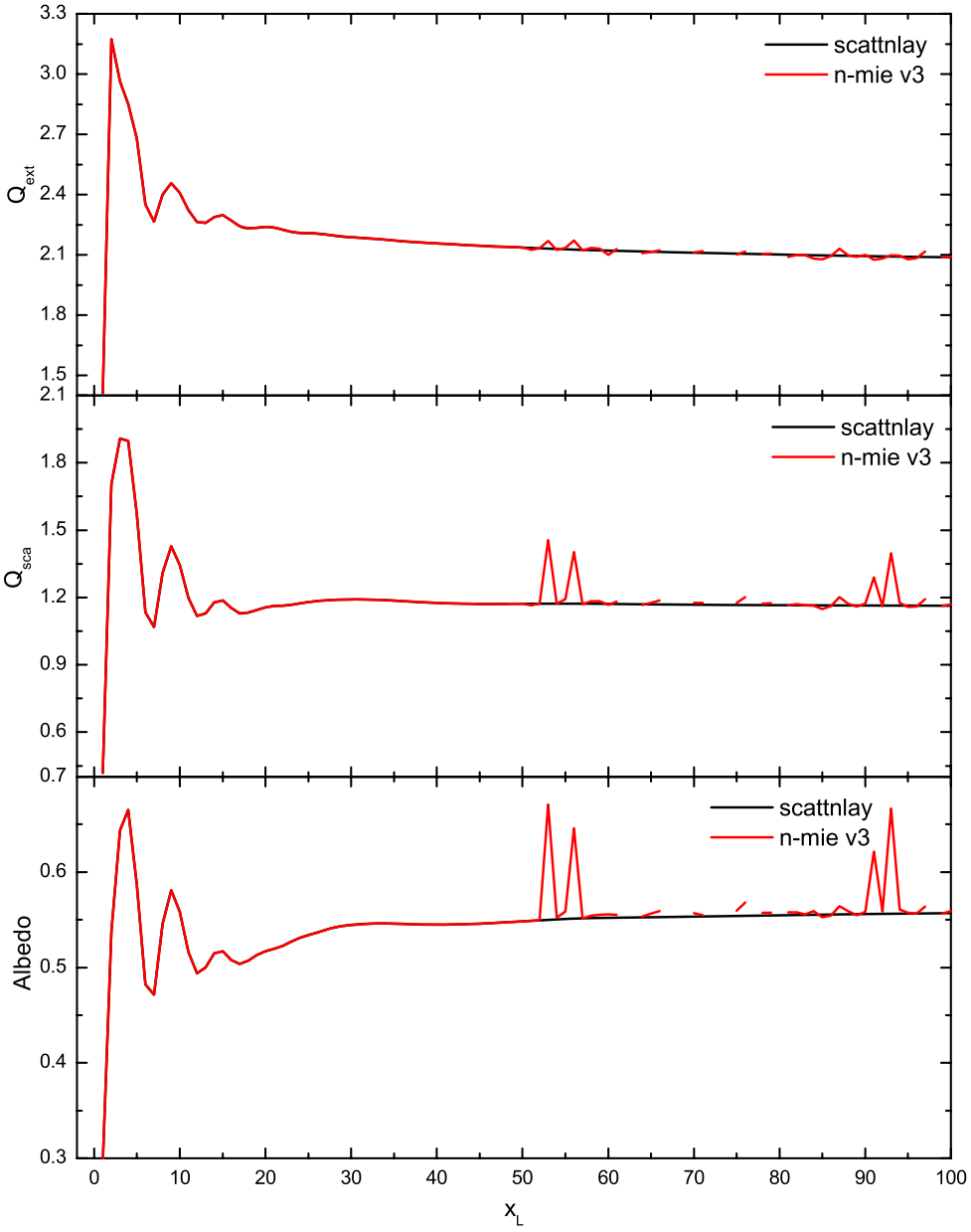

Fig. 1. Extinction and scattering efficiencies (Q_{ext}, Q_{sca}) and single-scattering albedo as the function of size parameter of the outermost layer for a 5-layer sphere with $m_1 = 1.8 + i1.7$, $m_2 = 0.8 + i0.7$, $m_3 = 1.2 + i0.09$, $m_4 = 2.8 + i0.2$, $m_5 = 1.5 + i0.4$, $V_1/V_T = 0.1$, $V_2/V_T = 0.26$, $V_3/V_T = 0.044$ and $V_4/V_T = 0.3666$.

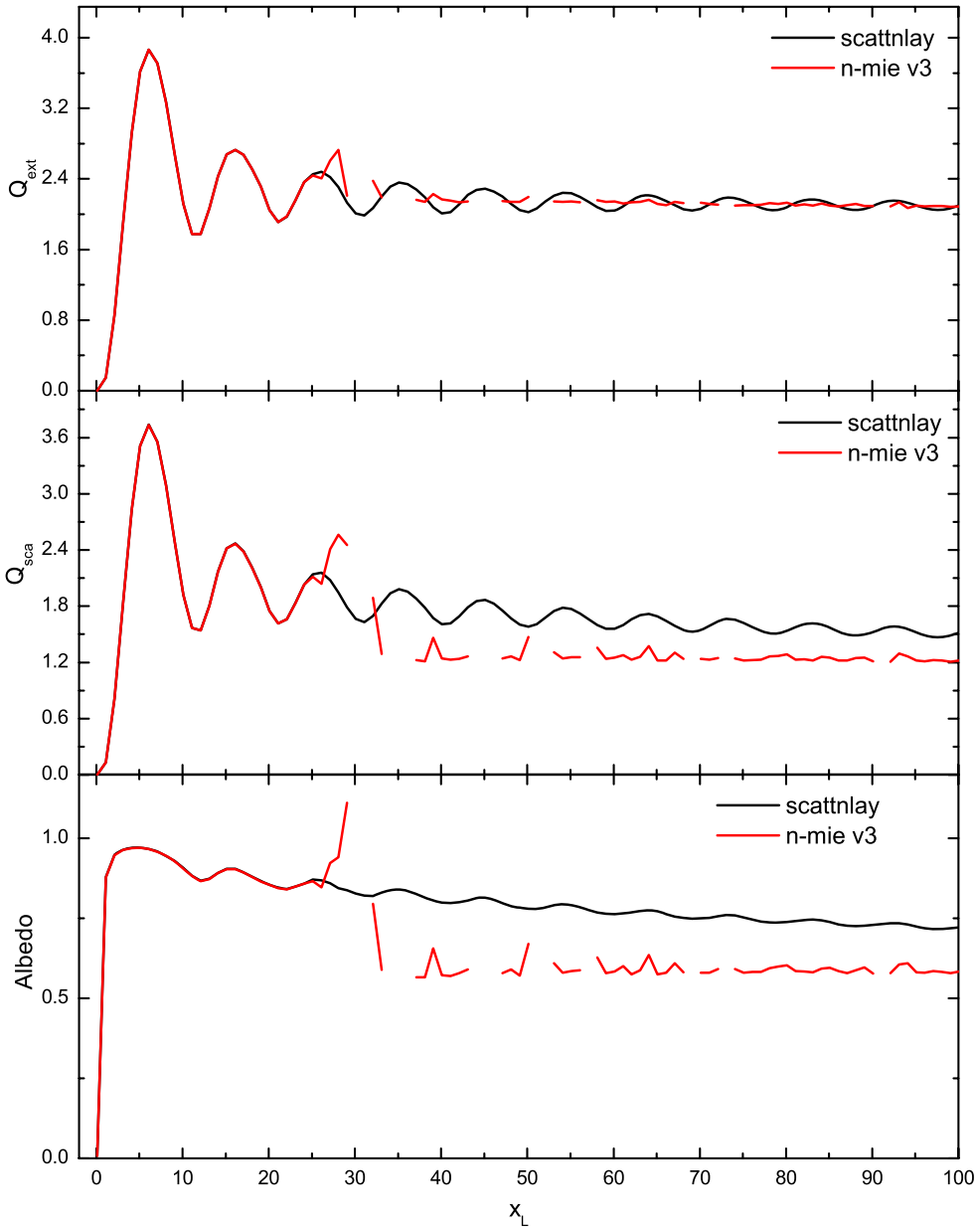

Fig. 2. Extinction and scattering efficiencies (Q_{ext}, Q_{sca}) and single-scattering albedo as the function of size parameter of the outermost layer for a soot-coated water sphere. The refractive indices of water and soot are $m_1 = 1.33 + i0.00$, $m_2 = 1.59 + i0.66$, respectively and the volume fraction of soot is 0.01.

differential scattering cross sections are calculated in the program but they can be easily obtained from Eqs. (24a)–(24d) and (34), respectively. The calculation finishes after the inclusion of N_{max} multipolar expansion terms in the calculation of the scattering coefficients.

3.1. Tests of the code

The accuracy of the code was tested for five different cases. For the first two of them, the results were compared with the ones obtained using the program *n-mie* version 3 [20], which implements the recursive algorithm developed by Wu and Wang [10], the applicability limits of the program are explored for the Kai and Massoli's model [13] in the third test and compared with results from the geometrical optics for the Luneburg lens (fourth case); finally, in the fifth test case the obtained values are compared with reported experimental results.

3.1.1. Five-layers sphere

The first test case uses the benchmark distributed with *n-mie* (a 5-layers sphere with $m_1 = 1.8 + i1.7$, $m_2 = 0.8 + i0.7$, $m_3 = 1.2 + i0.09$, $m_4 = 2.8 + i0.2$, $m_5 = 1.5 + i0.4$, $V_1/V_T = 0.1$, $V_2/V_T = 0.26$, $V_3/V_T = 0.044$ and $V_4/V_T = 0.3666$). The values of Q_{ext}, Q_{sca} and the albedo obtained for x_L between 1.0 and 100.0 can be observed in Fig. 1. For the values of x_L lower than 50.0, the results of both programs are in excellent agreement (4 decimal places). However, for values of x_L greater than 50.0, *n-mie* presents numerical problems and the results are obviously illogical. *scattnlay*, on the other hand, doesn't have any problem for the whole interval.

3.1.2. Soot-coated water sphere

The second test consists in a soot-coated water sphere, which was previously described by Yang [14] (the refractive indices of water and soot are $m_1 = 1.33 + i0.00$, $m_2 = 1.59 + i0.66$, respectively and the volume fraction of soot is *0.01*). Again Q_{ext}, Q_{sca} and

the albedo were obtained for x_L in between 1.0 and 100.0. For this extreme case [14] (Fig. 2), *n-mie* fails even earlier (for $x_L > 20.0$) while again *scattnlay* has no problem. For the region where *n-mie* is accurate ($x_L < 20.0$) the results of both programs are the same up to 5 decimal places.

3.1.3. Kai and Massoli's model

The applicability limits of our computer code were explored for the Kai and Massoli's model in the third test. The model consists in a multilayered sphere with a radial profile of the refractive index $m_l = n_l + ik_l$ given by $n_l = n_1 + 0.5(n_L - n_1)(1 - \cos t\pi)$ and $k_l = 0$, where $t = (l-1)/(L-1), n_1 = 1.01n_L$, and $n_L = 1.33$. The size parameter is $x_l = x_1 + t(x_L - x_1)$, where $l = 1, 2, \ldots, L$, $x_1 = 0.001x_L$ and L is the total number of layers. The obtained domain is shown in Fig. 3; it can be seen that a considerable improvement was obtained (when compared to Fig. 3, Ref. [14]).

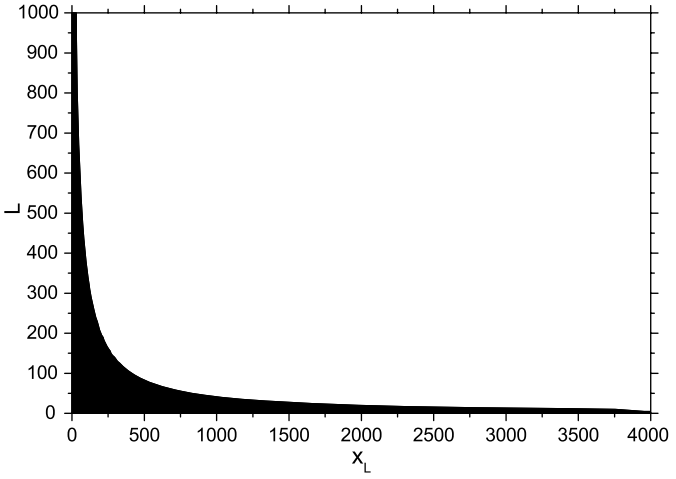

Fig. 3. Computational domain of our computer code for Kai and Massoli's model (black region). When compared with their computational domain (Fig. 3, Ref. [14]), it can be seen that a considerable improvement was obtained. The refractive index $m_l = n_l + ik_l$ is $n_l = n_1 + 0.5(n_L - n_1)(1 - \cos t\pi)$ and $k_l = 0$, where $t = (l-1)/(L-1)$, $n_1 = 1.01n_L$, and $n_L = 1.33$. The size parameter is $x_l = x_1 + t(x_L - x_1)$, where $l = 1, 2, \ldots, L$, $x_1 = 0.001x_L$ and L is the total number of layers.

3.1.4. Luneburg lens

This test case is the scattering from a Luneburg lens [11,14], which is a sphere of radius a with a radially-varying index of refraction, given by:

$$m(r) = \left[2 - \left(\frac{r}{a}\right)^2\right]^{1/2}. \tag{35}$$

For the calculations, the Luneburg lens was approximated as a multilayered sphere with 500 equally spaced layers. The refractive index of each layer is defined to be equal to $m(r)$ at the midpoint of the layer: $m_l = [2 - (\bar{x}/x_L)^2]^{1/2}$, with $\bar{x} = (x_{l-1} + x_l)/2$, for $l = 1, 2, \ldots, L$. The size parameter in the lth layer is $x_l = lx_L/500$. According to geometrical optics theory, the reduced differential cross section (the differential cross section divided by a^2) can be expressed as [11]:

$$dC_{sca}/d(a^2\Omega) = \cos(\theta). \tag{36}$$

This formula is valid in the angular range $0 \leqslant \theta \leqslant \pi/2$. No rays are scattered to angles larger than $\pi/2$ and therefore the geometric optics differential cross section of a Luneburg lens is zero in the range $\pi/2 \leqslant \theta \leqslant \pi$. The differential cross section was calculated from Eq. (34), considering that the expression is simplified if the incident light is unpolarized:

$$\frac{dC_{sca}}{d\Omega} = \frac{S_{11}(\theta)}{k^2}. \tag{37}$$

The results are shown in Fig. 4 for size parameter $x_L = 60$. The quantity plotted is the reduced differential cross sections $dC_{sca}/d(a^2\Omega)$. The obtained results accurately match those by Johnson [11] and Yang [14]. It can also be seen that for angles below $\pi/2$ and outside the forward scattering region, the wave optics differential cross section oscillates around the geometric optics value.

3.1.5. Experimental results

Finally, the values obtained by *scattnlay* were compared with experimental results. For this we used the normalized absorbance reported for gold nanoshells by Schwartzberg et al. [21]. The normalized values of Q_{ext} were obtained (Fig. 5) using the values of

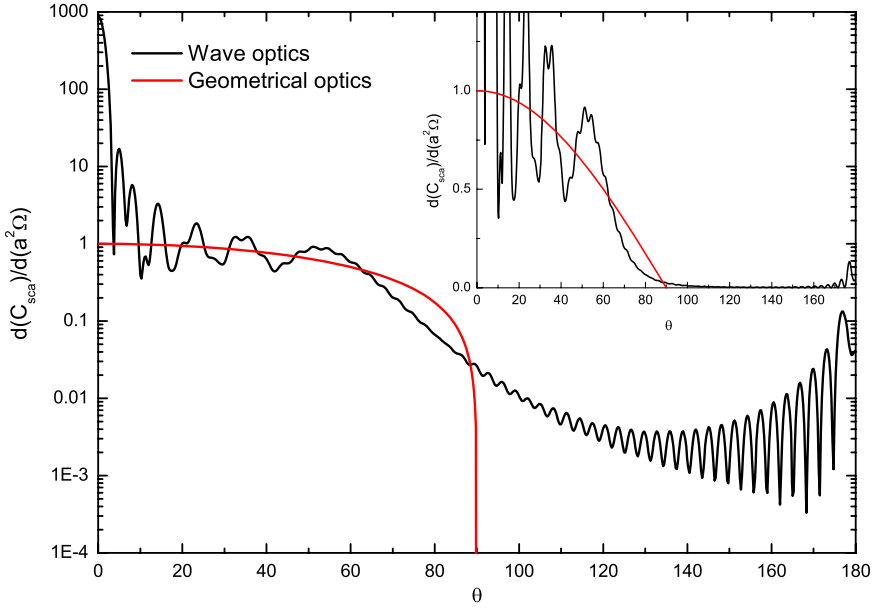

Fig. 4. Reduced differential cross section $dC_{sca}/d(a^2\Omega)$ as a function of scattering angle θ for a spherical Luneburg lens with a size parameter $x_L = 60$. The size parameter in the lth layer is $x_l = lx_L/500$. The refractive index is $m_l = [2 - (\bar{x}/x_L)^2]^{\frac{1}{2}}$, with $\bar{x} = (x_{l-1} + x_l)/2$, for $l = 1, 2, \ldots, L$. From the geometrical optics theory, $dC_{sca}/d(a^2\Omega) = \cos(\theta)$. The inset shows the same graph using a linear scale, instead of the logarithmic one used in the main graph.

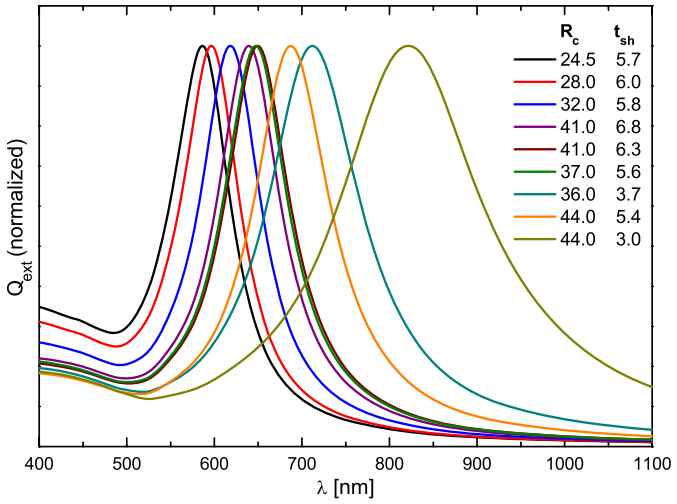

Fig. 5. Normalized Q_{ext} calculated using the values of R_c and t_{sh} reported in Ref. [21] for different nanoshells, and the refractive index of gold reported by Johnson and Christy [22].

R_c and t_{sh} reported in Ref. [21], for different nanoshells and the refractive index of gold was obtained from Johnson and Christy [22]. It can be noted that our results (Fig. 5) are in excellent agreement with the spectra in Fig. 4 of Ref. [21] in spite of the experimental errors and the size distribution that almost certainly exists in their samples.

4. Conclusions

The calculations performed using Mie theory have been for many years a powerful tool for better understanding the scattering of electromagnetic radiation. Although a lot of programs are publicly available for the case of scattering by a solid sphere, only a few of them are able to deal with a multilayered sphere and they have convergence problems for relatively low values of x_L. In this work we describe a computer implementation of the efficient algorithm developed by Yang [14] and showed that it is very accurate for a wide range of size parameters, considerably increasing the applicability limits with respect to equivalent computer codes. We also showed that the program is able to reproduce well experimental results. This implementation of Yang's algorithm, to our knowledge, would be the first of its kind to be available publicly.

Acknowledgements

The authors acknowledge the financial help of CONACyT, Mexico through the project # 46269. O. Peña is grateful to CONACyT, Mexico for extending a postdoctoral fellowship.

References

[1] L.R. Hirsch, R.J. Stafford, J.A. Bankson, S.R. Sershen, B. Rivera, R.E. Price, J.D. Hazle, N.J. Halas, J.L. West, Proc. Natl. Acad. Sci. USA 100 (2003) 13549–13554.
[2] Ch. Loo, A. Lowery, N. Halas, J. West, R. Drezek, Nano Lett. 5 (2005) 709–711.
[3] A.M. Gobin, M.H. Lee, N.J. Halas, W.D. James, R.A. Drezek, J.L. West, Nano Lett. 7 (2007) 1929–1934.
[4] P. Chylek, V. Ramaswamy, R.J. Cheng, J. Atmos. Sci. 41 (1984) 3076–3084.
[5] J.V. Martins, P. Artaxo, C. Liousse, J.S. Reid, P.V. Hobbs, Y.J. Kaufman, J. Geophys. Res. 103 (1998) 32041–32050.
[6] A.L. Aden, M. Kerker, J. Appl. Phys. 22 (1951) 1242–1246.
[7] J.R. Wait, Appl. Sci. Res. B 10 (1963) 441–450.
[8] R. Bhandari, Appl. Opt. 24 (1985) 1960–1967.
[9] D.W. Mackowski, R.A. Altenkirch, M.P. Menguc, Appl. Opt. 29 (1990) 1551–1559.
[10] Z.S. Wu, Y.P. Wang, Radio Sci. 26 (1991) 1393–1401.
[11] B.R. Johnson, Appl. Opt. 35 (1996) 3286–3296.
[12] Z.S. Wu, L.X. Guo, K.F. Ren, G. Gouesbet, G. Grehan, Appl. Opt. 36 (1997) 5188–5198.
[13] L. Kai, P. Massoli, Appl. Opt. 33 (1994) 501–511.
[14] W. Yang, Appl. Opt. 42 (2003) 1710–1720.
[15] K. Hasegawa, Ch. Rohde, M. Deutsch, Opt. Lett. 31 (2006) 1136–1138.
[16] V.E. Cachorro, L.L. Salcedo, J. Electromag. Waves Appl. 5 (1991) 913–926.
[17] W.J. Wiscombe, Appl. Opt. 19 (1980) 1505–1509.
[18] C.F. Bohren, D.R. Huffman, Absorption and Scattering of Light by Small Particles, Wiley, New York, 1983.
[19] M.I. Mishchenko, L.D. Travis, A.A. Lacis, Scattering, Absorption, and Emission of Light by Small Particles, Cambridge University Press, UK, 2002.
[20] N.V. Voshchinnikov, J.S. Mathis, Astrophys. J. 526 (1999) 257–264.
[21] A.M. Schwartzberg, T.Y. Olson, C.E. Talley, J.Z. Zhang, J. Phys. Chem. B 110 (2006) 19935–19944.
[22] P.B. Johnson, R.W. Christy, Phys. Rev. B 6 (1972) 4370–4379.